VEHICLE-TO-VEHICLE FULL FRONTAL CRASH OPTIMIZATION USING A CAE-BASED METHODOLOGY

Saeed Barbat, Xiaowei Li, Phillip Przybylo and Priya Prasad
Safety Research and Development
Ford Motor Company

ABSTRACT

This paper describes a CAE-based methodology used to identify major factors influencing vehicle structural performance and crash energy management in full-frontal vehicle-to-vehicle collisions. Finite element models of an "average" SUV and an "average" full-size passenger vehicle were used in this study. The determining factors of vehicle compatibility in multi-vehicle collisions are relative mass, relative stiffness and relative geometry. Four parameters of the average SUV, mass, fore rail length, fore rail thickness, and fore rail height were selected as design variables. A uniformly spaced Optimal Latin Hypercube sampling technique was employed to probe the design space of these variables using thirteen simulation runs.

Dash intrusions in the passenger vehicle and the absorbed collision energy in both vehicles were selected as response variables. Polynomial response surfaces were constructed, based on the simulation results, and found to fit the results well (R^2= 0.98 for dash intrusion and R^2= 0.85 for absorbed energy). As a result, prediction equations for maximum dash intrusion and absorbed collision energy as a function of the vehicle design variables were obtained. Results indicated that aligning front-end structures (specifically fore rail heights between impacted vehicles) in vehicle-to-vehicle full-frontal collisions has greater effect on reducing dash intrusions and managing crash energy than mass and variables associated with stiffness. An optimal design solution could also be determined with the appropriate introduction of constraint conditions.

INTRODUCTION

Vehicle compatibility has been investigated in many studies using different approaches such as real-world crash statistics, crash testing and computer modeling. Statistics from the General Estimates System (GES) were used to determine the number of vehicle-to-vehicle collisions [1]. One objective of these studies was to identify and demonstrate the extent of the problem of vehicle compatibility. Another objective was to demonstrate, through statistical analysis, the aggressivity metric as a function of vehicle mass, stiffness, and geometry. Other statistical analysis such as that conducted by Evans [2,3] indicated that mass is one of the most significant factors affecting potential risk of occupant injury in vehicle-to-vehicle collisions. His study indicated that the ratio of the injury rate in a lighter vehicle to that in a heavier one can be expressed as the power function of the mass ratio (of the heavier to the lighter vehicle). Accident data in Japan and computer modeling techniques were also used by Mizuno and Kajzer [4] to investigate the compatibility of mini cars in traffic accidents. Barbat, *et al.* [5,6] also investigated factors influencing compatibility in SUV/LTV-to-car crashes. Their study proposed a robust and repeatable vehicle-to-vehicle test procedure to help assess vehicle compatibility, and their preliminary results indicated that geometric compatibility was the dominant factor.

In addition to occupant responses, attempts have been made to characterize frontal crash performance with structural responses (i.e., occupant compartment intrusions and energy distribution) [5-8] in vehicle-to-vehicle collisions. Barbat, *et al*. [5,6] has shown the importance of occupant compartment intrusions in full-frontal SUV/LTV-to-car crashes. Steyer, *et al.* [7] postulated that frontal crash compatibility was dependent upon the distribution of collision energy absorbed in vehicle-to-vehicle crashes.

The consensus is that the significant parameters influencing compatibility in vehicle-to-vehicle crashes are geometric interaction, vehicle stiffness and vehicle mass. The effect of each individual design parameter, however, is not clearly understood. Separating the effects in various crash configurations via experimentation would not only be costly and time consuming, but also would be susceptible to systemic errors due to test-to-test variability. Because of the limitations of the statistical approach and crash testing, math modeling in combination with design of experiments (DOE) methods was deemed necessary to examine the influence of vehicle mass, stiffness, structural interaction and geometry on vehicle compatibility.

Finite element (FE) simulations have been used to study many aspects of vehicle crashworthiness.

Carefully designed experiments can characterize responses over the entire design space using a reduced number of simulations. The development of a FE model-based DOE methodology focused on discerning the effects of a few design variables on structural intrusions in 40% offset, car-to-car collisions has been previously presented by Brown, *et al*. [8] Brown's work revealed some of the economies of combining FE analysis and statistical techniques. The current study, while fundamentally similar, utilizes a deterministic approach that allowed analytical prediction equations for structural responses to be generated. This study combined FE analysis, Latin Hyper Cube Sampling (LHS), and subset selection with sequential replacement to produce a powerful tool that may be used to investigate vehicle compatibility issues. A full-frontal, collinear, SUV-to-passenger vehicle crash configuration (See Figure 1) was used in this study. This technique can also be extended to various crash configurations other than the one used in this study.

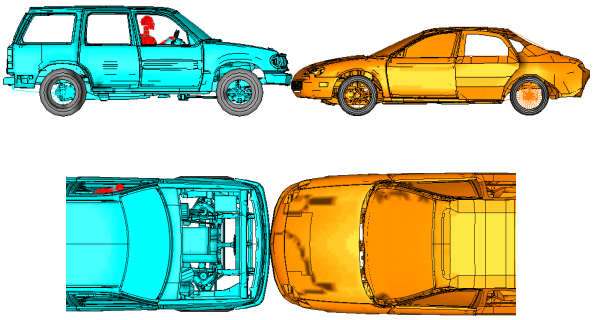

Figure 1. Baseline model of SUV-to-passenger vehicle full-frontal crash simulation.

SYSTEM SETUP

Finite Element Modeling

Reliable finite element models of the vehicles are required to enable reasonable predictions of structural performance. In this study, full-vehicle finite element models validated to rigid barrier tests were used for the "average" SUV and the "average" passenger vehilce. A baseline, full-frontal vehicle-to-vehicle FE model was constructed by combining the two vehicle models and it was correlated to a physical vehicle-to-vehicle full-frontal crash test. As in the physical test, the simulated passenger vehicle was stationary and the simulated SUV was given an initial velocity of 96 km/h.

Full-frontal, collinear SUV-to-passenger vehicle simulations involve many complex and non-linear interactions. The nonlinear, explicit FE crash code, RADIOSS [9], was used for all of the simulations. The appropriate selection of design variables and their levels as well as, the pertinent system responses are basic requirements.

Design Variable Selection

It is generally accepted that the determining factors of vehicle compatibility are relative geometry, relative stiffness and relative mass. All three factors were considered here through four design variables, the SUV fore rail height, fore rail length, fore rail thickness, and mass. Geometric differences between the SUV and the passenger vehicle were modeled as relative vertical alignment between the fore-most structural members in each vehicle. The SUV front-end stiffness was separated into two design variables, fore rail length and fore rail thickness. This separation allows the effects of the design variables to be interpreted independently and to be associated with vehicle characteristics. For each design variable, only the SUV portions of the FE models were changed to reflect the respective ranges. A brief description of how the variables were introduced into the FE models and the levels selected for the design variables follows.

Geometry

The vertical alignment of load-bearing/energy-absorbing structures was varied to allow geometric effects to be observed. The relative vertical offsets were accomplished by changing the ground reference plane of the SUV with respect to that of the passenger vehicle. The four discrete levels selected are depicted in Figure 2.

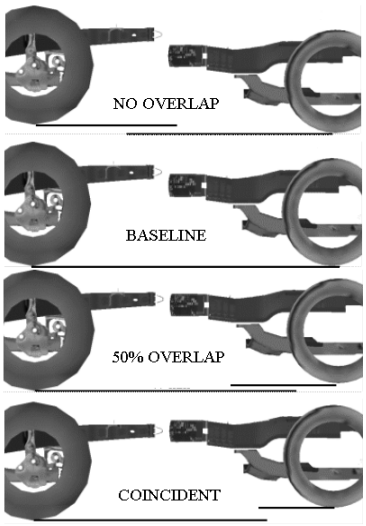

Figure 2. Geometric design variable implementation.

The BASELINE configuration, NO OVERLAP between the fore rails, 50% OVERLAP of the PASSENGER VEHICLE fore rail, and COINCIDENT FORE RAIL centerlines were included in the study. The range of levels encompass from a potentially overriding condition to an aligned configuration.

Modeling the geometric changes in this manner shifts the center of gravity height of the SUV. The effect this amount of the shift would have on the overall responses of the vehicles was considered minimal.

Stiffness

The relative stiffness was modeled with two design variables, SUV fore rail length and SUV fore rail thickness. The length of the fore rail was modeled at four discrete levels, baseline (average SUV), +25 mm, +50 mm and +75 mm. Models associated with each design level are shown in Figure 3. In addition to adjusting the fore rail length, components such as the bumper system, radiator, and light supports were translated in the longitudinal direction by appropriate amounts.

The second stiffness-related deign variable was the SUV fore rail wall thickness. As with the two previous design variables, the thickness was studied at four distinct levels, baseline, -0.5 mm, -1.0 mm, and +0.5 mm.

Mass Ratio

The final design variable studied was the ratio of the SUV mass to the passenger vehicle mass, hereafter referred to as mass ratio. In order to vary the mass ratio, the SUV mass was adjusted by distributing small masses throughout the model such that the center of gravity location remained equivalent to the BASELINE location. The mass of the SUV was varied from BASELINE-20% to BASELINE+20% in 10% increments. The range approximately spans the vehicle segments from small SUV to large SUV. The corresponding mass ratios ranged from 0.9 to 1.38 in five discrete levels (see Table 1). Since the initial velocity of the SUV was the same for all simulations, the velocity change (ΔV) experienced by each vehicle varied with the mass ratio. Table 1 shows the ΔV's experienced by the vehicles at the various mass ratios. The velocity change is an indicator of the crash severity commonly used for vehicle crashes.

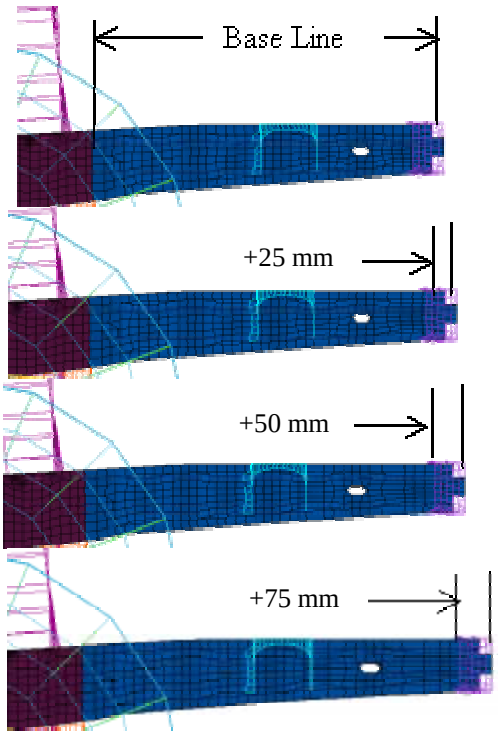

Figure 3. SUV fore rail length.

Table 1.
Passenger Vehicle and SUV Velocity Changes

Mass Ratio	Passenger Vehicle ΔV [km/h]	SUV ΔV [km/h]
0.90	45.7	50.9
1.02	48.8	47.8
1.14	51.5	45.1
1.26	53.9	42.6
1.38	56.0	40.6

Table 2 contains a summary of the design variables and their corresponding levels. The levels have been associated with an integer representation (coded) for simplicity.

Table 2.
Summary of Coded Design Variables and Levels

Fore Rail Height
1 = No overlap
2 = BASELINE 3 = 50% Overlap of PASSENGER VEHICLE fore rail
4 = Coincident
Fore Rail Length
1 = BASELINE
2 = BASELINE + 25 mm
3 = BASELINE + 50 mm
4 = BASELINE + 75 mm
Fore Rail Thickness
1 = BASELINE – 1.0 mm
2 = BASELINE – 0.5 mm
3 = BASELINE
4 = BASELINE + 0.5 mm
Mass
1=BASELINE – 20%
2=BASELINE – 10%
3= BASELINE
4= BASELINE + 10%
5= BASELINE + 20%

System Responses

Occupant compartment intrusion is a metric, which is used in comparative studies of vehicle crash performance (e.g., the Insurance Institute for Highway Safety includes occupant compartment intrusion in their evaluation of vehicles in a 64 km/h 40% offset deformable barrier crash test). In this study, several passenger vehicle intrusions and the vehicles' collision energy management were the responses of interest (see Table 3).

The toe board intrusions were measured along the driver and passenger centerline on the dash, 200 mm up from the floor panel. The windshield intrusions were taken at the intersection between the lower edge of the windshield and the cowl at the windshield centerline. The driver and passenger A-pillar intrusions were monitored near the juncture between the lower windshield, the A-pillar, and the cowl. Bumper to rocker crush was taken as the relative longitudinal displacement between the bumper beam center and rocker at the B-pillar. The maximum dash intrusion was captured from a vertical section along the dash from the cowl to the floor through the driver centerline. The intrusions were calculated as the relative displacement between the point of interest and a reference point located on the rocker at the B-pillar.

Table 3.
Selected Responses

Passenger Vehicle
Driver Toe board Intrusion
Driver A-pillar Intrusion
Lower Windshield Center Intrusion
Passenger A-pillar Intrusion
Passenger Toe board Intrusion
Bumper to Rocker Crush
Driver Centerline Dash Intrusion
Internal Energy Absorbed
SUV
Internal Energy Absorbed

The distribution of collision energy absorbed between the vehicles was also a response monitored in this study. The internal energies absorbed that were calculated from the FE simulations are reported.

EXPERIMENTAL DESIGN

The number of factors and levels included in this study describe a sizable design space. Numerous techniques exist for constructing experimental designs that specify a minimal number of samples throughout the design space to characterize the responses [10,11]. Latin Hypercube Sampling was utilized to select the design levels for the FE models due to its ability to uniformly sample the design space and its flexibility in the number of levels for each design variable. Since no noise factors were introduced into this study, the minimum number of simulations to construct a reasonably accurate response surface was 12 (3N where N is the number of control factors). The outcome of the sampling process is shown in Table 4. One additional run was included in the matrix to represent the baseline simulation that was correlated to a physical test. All 13 simulations were conducted for 150 ms.

Table 4.
Simulation Matrix

	Fore Rail Height	Fore Rail Length	Fore Rail Thickness	Mass
1 (Base line)	*2*	*1*	*3*	*3*
2	4	4	2	2
3	2	4	3	4
4	4	2	3	3
5	1	1	3	1
6	3	1	1	2
7	1	4	1	3
8	4	3	1	5
9	2	2	2	5
10	3	3	4	1
11	2	3	2	1
12	1	2	4	4
13	3	1	4	5

Finite Element Simulation Results

Table 5 contains the responses from the FE simulations. All intrusion responses were normalized with respect to the intrusions associated with the baseline simulation. The energy absorbed in both vehicles was computed and reported as the ratio of the energy absorbed in the passenger vehicle to that absorbed in the SUV. Response surfaces were created to allow interpretation over the design space and efficient (FE model-free) studies to be carried out.

Table 5.
Normalized Simulation Responses

	Driver A-Pillar	Wind-shield	Passenger A-Pillar	Driver Toe board	Passenger Toe board	Bumper To Rocker	Maximum Dash Intrusion	IE Ratio
1	1	1	1	1	1	1	1	2.6
2	0.41	0.31	0.47	0.63	0.78	0.81	0.43	1.5
3	1.17	1.28	1.31	1.17	1.19	0.99	1.16	2.3
4	0.64	0.40	0.68	0.76	0.86	0.83	0.51	1.8
5	0.59	0.71	0.71	1.20	0.86	0.95	0.94	1.9
6	0.57	0.50	0.60	0.78	0.77	0.86	0.50	1.7
7	0.70	1.08	0.97	1.25	0.98	1.07	1.09	1.8
8	1.11	0.68	0.86	0.84	0.78	1.00	0.79	1.5
9	1.07	1.17	1.13	1.23	1.21	1.08	1.10	2.0
10	0.77	0.54	0.71	0.47	0.83	0.80	0.51	2.5
11	0.57	0.62	0.73	0.83	0.81	0.84	0.73	2.0
12	1.26	1.33	1.32	1.39	1.11	1.04	1.28	2.7
13	1.18	1.05	1.22	0.96	1.10	0.96	0.96	2.4

Response Surface Generation

The sample responses obtained from the FE simulations (Table 5) were fit with quadratic polynomials using regression based upon subset selection by sequential replacement. Gu [11] showed that for structural intrusions and internal energy predictions in crash applications, quadratic polynomials are often sufficient. The polynomial basis of the equations allows the response surface dependency on the design variables to be interpreted by observation. Furthermore, the explicit form of the response surfaces lends itself to a variety of design studies (e.g., parameter sensitivity analysis or optimization). The coefficient of determination, referred to symbolically as R^2, is a measure of the model's ability to fit the response data and was used to identify the best-fit equations in the least squares sense.

The response surfaces and R^2 values for the fit polynomials are listed in Table 6. In the response surface expressions, H is the SUV fore rail height, L is the SUV fore rail length, T is the SUV fore rail thickness, M is the mass ratio, and a_1-a_8, b_1-b_8, c_1-c_8, d_1-d_8, and e_1-e_8 are the best fit coefficients. The R^2 values shown in the table indicate that the response surfaces are capable of representing the sampled FE results.

Table 6.
Response Surfaces and R^2

Response Surface	R^2
Driver Toeboard Intrusion $= a_1 - b_1 H M - c_1 T^2 + d_1 T + e_1 M$	0.94
Drive A Pillar Intrusion $= a_2 + b_2 M - c_2 T H - d_2 T M + e_2 T^2$	0.87
Windshield Intrusion $= a_3 - b_3 H^2 + c_3 L T - d_3 M^2 + e_3 M$	0.99
Passenger A Pillar Intrusion $= a_4 + b_4 T M + c_4 L T - d_4 H^2 + e_4 M$	0.97
Passenger Toeboard Intrusion $= a_5 - b_5 H M - c_5 T^2 + d_5 T + e_5 M$	0.9
Bumper to Rocker Crush $= a_6 - b_6 T M + c_6 T - d_6 H + e_6 M$	0.96
Maximum Dash Intrusion $= a_7 - b_7 H^2 + c_7 L M + d_7 T - e_7 L T$	0.98
Energy Ratio $= a_8 + b_8 L M + c_8 T^2 - d_8 H^2 + e_8 H$	0.85

Verification of Equations

Four additional FE simulations were run to confirm the predictive character of the response surfaces. This step is not required in a rigorous mathematical sense, but it was conducted because of the complex nature of the crash mode. The parameters for these additional simulations were selected randomly from within the ranges of each design variable and the levels are shown in Table 7.

Table 7.
Verification Simulation Design Variable Levels

	Fore Rail Height	Fore Rail Length	Fore Rail Thickness	Mass
14	4	1	2	3
15	2	3	1	5
16	1	2	1	1
17	1	1	4	4

Figure 4 shows a bar chart comparing the FE simulation results and the predicted responses for passenger vehicle maximum dash intrusion. The run numbers from one through 13 correspond to the responses that were used to form the response surface. The remaining runs, run numbers 14 through 17, are the verification runs. The figure shows that the passenger vehicle maximum dash intrusion can be described via the prediction equation. The response surface, therefore, can be utilized for additional studies of designs contained within the original design space.

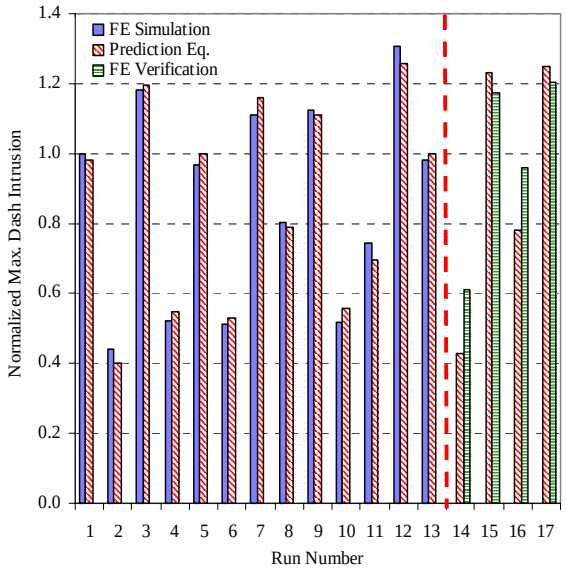

Figure 4. Normalized Passenger Vehicle Maximum Dash Intrusion

Figure 5 compares FE-simulated and predicted internal energy ratio responses for all runs previously described. The internal energy ratio response equation accurately predicted the responses for the additional runs. As with the maximum dash intrusion equation, the internal energy equations can be used to study the design space without conducting additional finite element simulations.

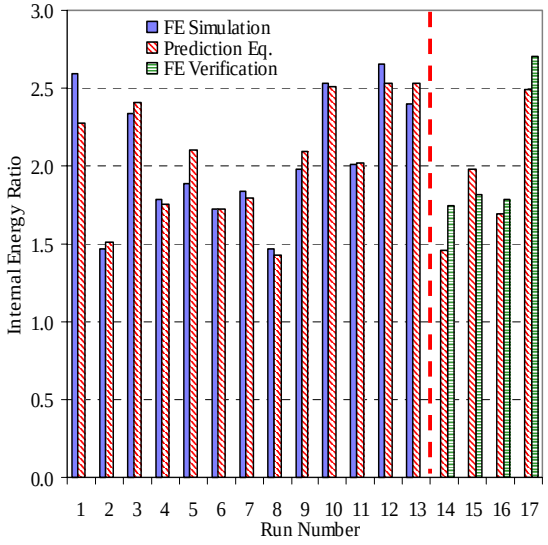

Figure 5. Internal Energy Ratio

RESULTS

Pair-wise Comparison of Design Variable Effects on Passenger Vehicle Maximum Dash Intrusion

Pair-wise comparisons of the predicted effects of the design variables show the relative importance of each factor. For all comparisons described, the variables that are not included were set to their BASELINE levels.

The comparison of the mass effect to the geometric and fore rail thickness effects on the passenger vehicle maximum dash intrusion (MDI) are shown in Figures 6 and 7, respectively. Figure 6 indicates that the MDI increases as the mass ratio increases while it decreases as the overlap percentage of the energy absorbing members of both impacted vehicles increases. Figure 6 also shows that fore rail height influences MDI more than the mass ratio for BASELINE stiffness SUV. That is, for a constant mass, the change in MDI due to changes in SUV fore rail height is greater than the change in MDI due to a change in the mass ratio for a constant fore rail height. This is also apparent from the contours of MDI.

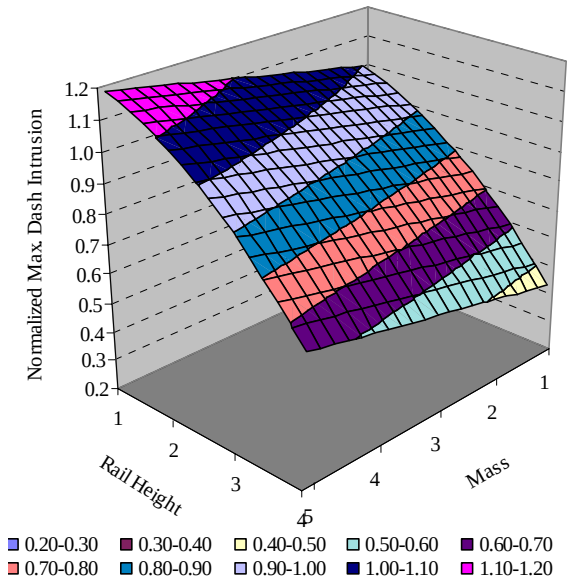

Figure 6. Mass-geometry surface plot of passenger vehicle maximum dash intrusion.

Figure 7 indicates that the MDI increases as the fore rail thickness and mass ratio increases. However, Figure 7 also shows that for BASELINE fore rail height and fore rail length, the fore rail thickness effect on MDI is larger than the mass ratio effect.

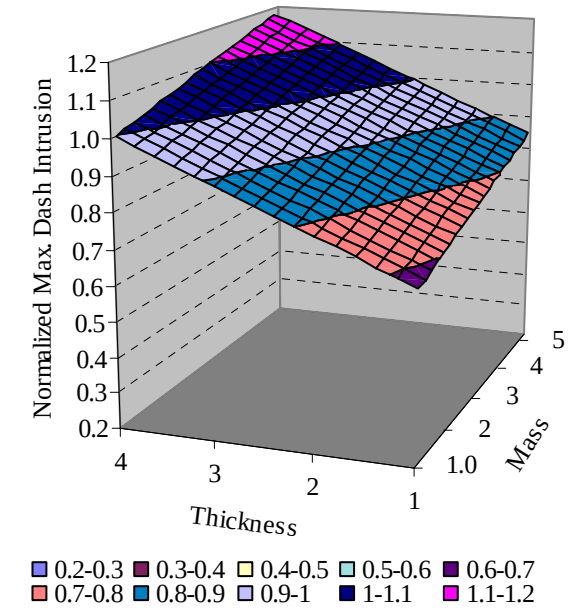

Figure 7. Mass-thickness surface plot of passenger vehicle maximum dash intrusion.

Figure 8 shows the comparison of the geometric effect to the thickness effect for BASELINE mass ratio and SUV fore rail length. The inclination of the surface indicates that the geometry effect is more than the thickness effect for MDI.

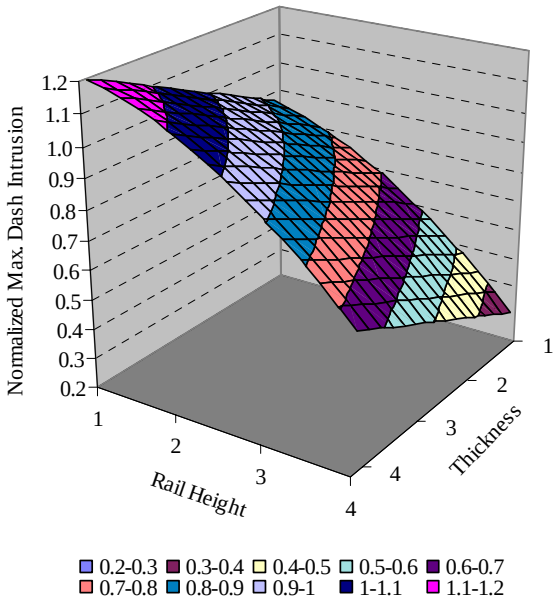

Figure 8. Geometry-thickness surface plot of passenger vehicle maximum dash intrusion.

The response surfaces in Figures 6 – 8 reveal that the geometric factor, relative fore rail height, has a greater effect than the relative mass and stiffness on the passenger vehicle maximum dash intrusion. These figures also showed that the thickness effect is more prominent than the mass effect.

Pair-wise Comparison of Design Variable Effects on Internal Energy Absorbed

Pair-wise comparisons of the effects of the design variables for internal energy absorbed ratio (IEAR) follow in Figures 9 through 11. Figures 9 and 10 contain comparisons of the mass ratio effect to the geometric and thickness effects on the IEAR, respectively. The geometric effect is compared to the thickness effect in Figure 11.

Figure 9 shows that the geometric effect on IEAR is much greater than the mass ratio effect. In fact, for the ranges considered the mass effect on IEAR is small (> 10%). For SUV fore rail height at level 1, the IEAR is lower than at SUV fore rail height level 2. Two possible explanations for this are: 1) structural components other than the fore rails of the vehicles are interacting or 2) the IEAR prediction equation is not accurate for this portion of the design space.

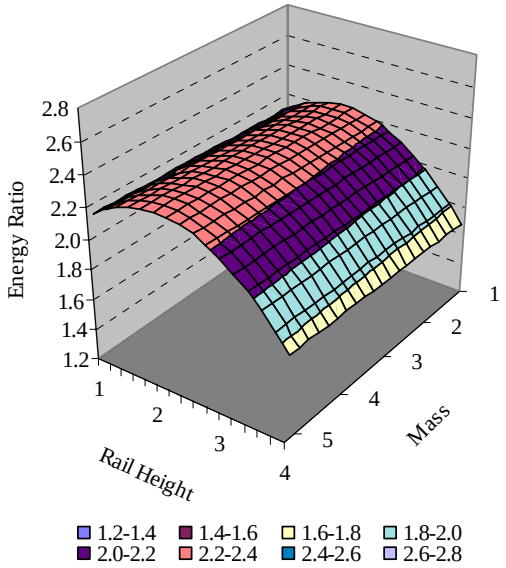

Figure 9. Geometry-mass surface plot of internal energy absorbed ratio.

Figure 10 contains the comparison of the mass ratio effect on IEAR to that of the SUV fore rail thickness. SUV fore rail thickness has a greater effect on IEAR than the mass ratio.

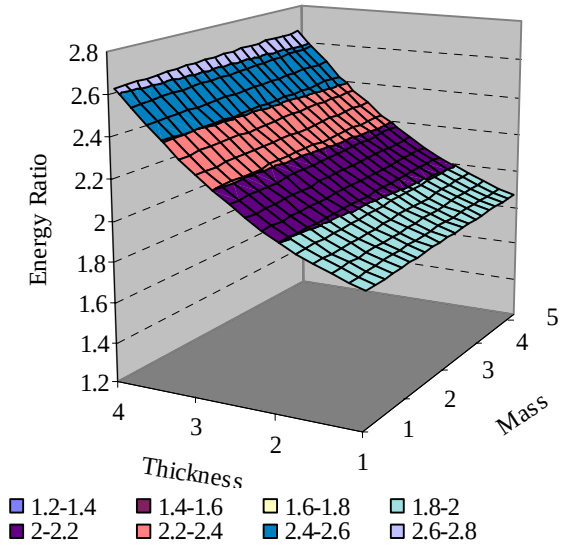

Figure 10. Mass-stiffness surface plot of internal energy absorbed ratio.

From Figure 11, the effects of SUV fore rail height and thickness can be seen. For IEAR the SUV fore rail height has a greater effect than thickness for SUV fore rail height levels 2 and higher. The thickness effect exceeds the height effect for the SUV fore rail height level 1 (i.e., NO OVERLAP/SUV over-ride condition). This switching of effect significance is subject to the explanations issued for Figure 9.

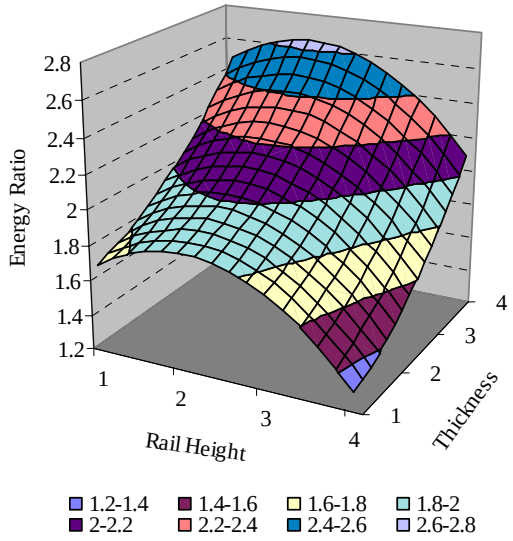

Figure 11. Geometry-stiffness surface plot of internal energy absorbed ratio.

RESPONSE OPTIMIZATION

Due to the predictive capability of the response surfaces, optimization can be performed on this set of surrogate models. The Safety Optimization and Robustness (SOAR) methodology developed by Yang, et al. [10] was the optimization technique applied. The explicit form of the response surfaces simplified the incorporation of the responses as objective or constraint functions. The objective function could be any of the response surfaces, but was chosen to minimize the passenger vehicle maximum dash intrusion subject to the constraints listed in Table 8. Since the optimal configuration depends on the constraint conditions, their magnitudes were based on the FE-simulated passenger vehicle responses taken from a rigid, fixed barrier (RFB) simulation at 56 km/h. That is, the intrusions in the optimal vehicle-to-vehicle full frontal simulation were limited to being no greater than the passenger vehicle striking itself. The internal energy ratio was restricted to being less than or equal to the BASELINE full-frontal vehicle-to-vehicle simulation.

A comparison of the optimized design to the BASELINE design follows. Figure 12 shows the comparison of passenger vehicle intrusions, and Figure 13 shows the internal energy absorption ratios. All intrusions into the passenger vehicle occupant compartment were reduced by at least 35% when

compared to the BASELINE simulation. The distribution of absorbed energy between the SUV and passenger vehicle was more balanced in the optimal configuration. These structural metrics indicate that this configuration (fore rail height = 4, fore rail length = 1, fore rail thickness = 1, mass ratio = 1) is more compatible for the full-frontal, collinear crash mode. The SUV described by the optimal configuration was the lightest, least stiff, and most aligned vehicle in the design space. This optimal design is based on only this test mode. However, this is a demonstration of the optimization technique capability and the optimum design needs to be further studied to ensure no degradation in self-protection.

Table 8.
Constraint Conditions

Response	Constraint
Driver A-pillar Intrusion	≤ *RFB*
Windshield Low Intrusion	≤ *RFB*
Passenger A-pillar Intrusion	≤ *RFB*
Driver and Passenger Toe board Intrusion	≤ *RFB*
Bumper to Rocker Deformation	≤ *RFB*
Internal Energy Ratio	≤ *BASELINE*

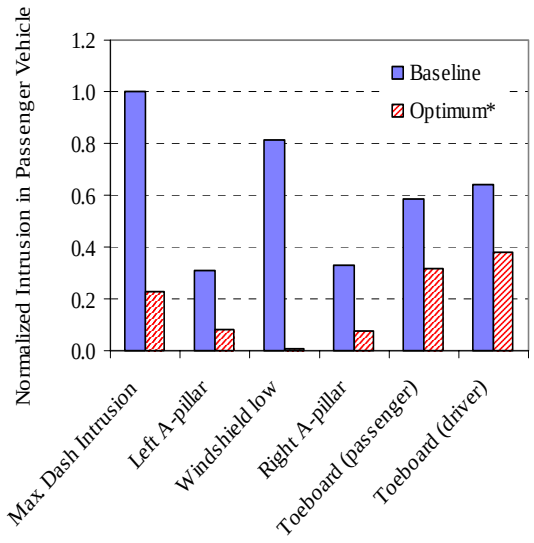

Figure 12. Passenger vehicle maximum dash intrusion – BASELINE vs. optimal.

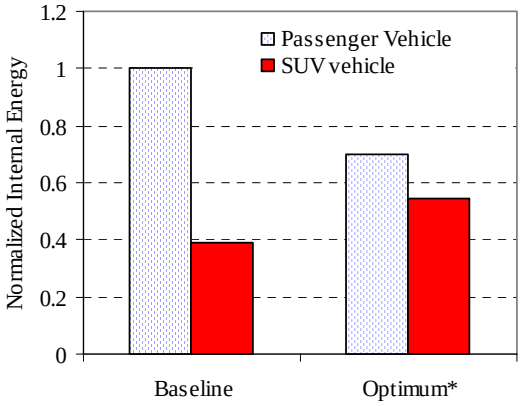

Figure 13. Internal energy absorbed.

SUMMARY

Validated finite element models of an "average" SUV and an "average" passenger vehicle were used to explore the effects of geometry, stiffness and mass in full-frontal collinear vehicle-to-vehicle collisions. Four design variables, the SUV fore rail height, fore rail length, fore rail thickness, and mass were chosen. Since this study was focused on structural performance and did not investigate the relationship between the structural responses and occupant responses, only passenger vehicle intrusions and vehicles' collision energy absorbed were selected as the responses.

A design of experiments methodology involving Latin Hypercube sampling was employed to select the appropriate number of simulations and the design levels of each of the design variables that should be incorporated in each simulation. The responses were characterized by quadratic polynomial surfaces. This characterization of the response surfaces could be done with higher order polynomials or other functions, but was not deemed necessary for this study based on the findings of Gu [11]. Four verification simulations showed that the response surfaces were adequate to capture the responses.

Pair-wise comparisons of the effects of the design variables were used to assess their individual influence on maximum dash intrusion and absorbed internal energy ratio. The pair-wise comparisons were based on the response surfaces generated from the 13 initial FE simulations. When a pair of design variables was compared, the remaining design variables were set to their BASELINE levels. In full-frontal, collinear SUV-to-passenger vehicle collisions, the relative geometric effect on maximum dash intrusion was greater than the mass and thickness effects. In addition, the thickness effect was

greater than the mass effect for this response. The test data of Barbat, *et al*. [5] also showed that the geometric effect was the most significant in full-frontal, collinear SUV/LTV-to-car collisions.

For this crash mode and the constraints imposed on the design, the optimal SUV vehicle configuration based upon minimization of passenger vehicle maximum dash intrusion had aligned fore rails, BASELINE mass – 20%, and BASELINE fore rail thickness – 1.0 mm. This configuration represented the best aligned, lightest, and least stiff SUV in the study.

More importantly, the effect of reducing the front-end stiffness of an SUV on self protection is not investigated in this study. This effect may degrade the structural and occupant performances in single vehicle accidents. Therefore, compatibility is a fleet-wide issue and design changes such as stiffness and geometry may involve real-world tradeoffs.

The methodology described can be applied to other crash configurations. In fact, several configurations could be considered simultaneously using this method.

CONCLUSIONS

- In full-frontal, collinear SUV-to-passenger vehicle collisions, the relative geometric effect on maximum dash intrusion was greater than the mass and thickness effects.
- The thickness effect was greater than the mass effect on maximum dash intrusion.
- Quadratic polynomial surfaces can characterize the structural intrusions for full-frontal, collinear SUV-to-passenger vehicle collisions.
- The optimal SUV vehicle configuration based upon minimization of passenger vehicle maximum dash intrusion had aligned fore rails, BASELINE mass – 20%, and BASELINE fore rail thickness – 1.0 mm.

REFERENCES

[1] Gabler, H.C. and W.T. Hollowell, "The Aggressivity of Light Trucks and Vans in Traffic Crashes", SAE Paper No. 980908, Detroit, 1998.

[2] Evans, L. and M.C. Frick, "Mass Ratio and Relative Driver Fatality Risk in Two-Vehicle Crashes", Accident Analysis and Prevention, Volume 25, pp 213-214, 1993.

[3] Evans, L., "Driver Injury and Fatality Risk in Two-Car Crashes versus Mass Ratio Inferred Using Newtonian Mechanics", Accident Analysis and Prevention, Volume 26, No.5, pp 609-616, 1994.

[4] Mizuno, K. and J. Kajzer, "The Compatibility of Mini Cars in Traffic Accidents", 16th ESV Conf., Paper No. 98-S3-O-08, Windsor, Canada, 1998.

[5] Barbat, S., X. Li, and P. Prasad, "A Comparative Analysis of Vehicle-to-Vehicle and Vehicle-to-Rigid Fixed Barrier Frontal Impacts", 17th ESV Conf., Paper No. 01-S7-O-01, Amsterdam, Netherlands, 2001.

[6] Barbat, S., X. Li and P. Prasad, "Evaluation of Vehicle Compatibility in Various Frontal Impact Configurations", 17th ESV Conf., Paper No. 01-S7-O-09, Amsterdam, Netherlands, 2001.

[7] Steyer, C., M. Delhommeau, and P. Delannoy, "Proposal to Improve Compatibility in Head on Collision", 16th ESV Conf., Paper No. 98-S3-O-05, Windsor, Canada, 1998.

[8] Brown, G. , E. Arvelo and A. Strong, "Investigation of the Major Factor Influencing Front Compatibility Design of Vehicles", SAE Paper No. 2001-01-1166, Detroit, 2001.

[9] RADIOSS Crash Guidelines, Mecalog SARL, 1997.

[10] Yang, R.J., A. Akkerman, D.F. Anderson, O.M. Faruque, and L. Gu, "Robustness Optimization for Vehicular Crash Simulations", Computing in Science and Engineering, pp. 8-13, Nov./Dec. 2000.

[11] Gu, L., "A Comparison of Polynomial-based Regression Models in Vehicle Safety Analysis", ASME 2001 DETC, Paper No. DAC-21063, Pittsburgh, 2001.